01 Mar 2013

Response Surface Method based on Radial Basis Functions for Modeling Large-Scale Structures in Model Updating

Linren Zhou

Guirong Yan
Missouri University of Science and Technology, yang@mst.edu

Jinping Ou

Recommended Citation

L. Zhou et al., "Response Surface Method based on Radial Basis Functions for Modeling Large-Scale Structures in Model Updating," *Computer-Aided Civil and Infrastructure Engineering*, vol. 28, no. 3, pp. 210 - 226, Wiley, Mar 2013.
The definitive version is available at https://doi.org/10.1111/j.1467-8667.2012.00803.x

Computer-Aided Civil and Infrastructure Engineering **28** (2013) 210–226

Response Surface Method Based on Radial Basis Functions for Modeling Large-Scale Structures in Model Updating

LinRen Zhou

School of Civil Engineering, Dalian University of Technology, Dalian, 116024, P. R. of China

GuiRong Yan

School of Civil Engineering, University of Texas at El Paso, El Paso, TX, USA

&

JinPing Ou*

School of Civil Engineering, Dalian University of Technology, Dalian, 116024, P. R. of China

Abstract: *The response surface (RS) method based on radial basis functions (RBFs) is proposed to model the input–output system of large-scale structures for model updating in this article. As a methodology study, the complicated implicit relationships between the design parameters and response characteristics of cable-stayed bridges are employed in the construction of an RS. The key issues for application of the proposed method are discussed, such as selecting the optimal shape parameters of RBFs, generating samples by using design of experiments, and evaluating the RS model. The RS methods based on RBFs of Gaussian, inverse quadratic, multiquadric, and inverse multiquadric are investigated. Meanwhile, the commonly used RS method based on polynomial function is also performed for comparison. The approximation accuracy of the RS methods is evaluated by multiple correlation coefficients and root mean squared errors. The antinoise ability of the proposed RS methods is also discussed. Results demonstrate that RS methods based on RBFs have high approximation accuracy and exhibit better performance than the RS method based on polynomial function. The proposed method is illustrated by model updating on a cable-stayed bridge model. Simulation study shows that the updated results have high accuracy, and the model updating based on experimental data can achieve reasonable physical explanations. It is demonstrated that the proposed approach is valid for model updating of large and complicated structures such as long-span cable-stayed bridges.*

*To whom correspondence should be addressed. E-mail: *oujinping@dlut.edu.cn.*

DOI: 10.1111/j.1467-8667.2012.00803.x

1 INTRODUCTION

In the past two decades, considerable attention has been attracted to structural health monitoring (Adeli and Jiang, 2009; Hampshire and Adeli, 2000; Ou, 2004; Park et al., 2007; Ou and Li, 2010; Xia et al., 2011), structural system identification (Jiang and Adeli, 2005; Adeli and Jiang, 2006; Jiang et al., 2007; Gangone et al., 2011; Jiang and Adeli, 2008a, b; Adeli and Kim, 2009), and damage identification (Jiang and Adeli, 2007; Li et al., 2011a; Li et al., 2011b; Jafarkhani and Masri, 2011; Talebinejad et al., 2011; Qiao et al., 2012; Xiang and Liang, 2012), which aim at developing a mathematical model, monitoring the performance of structures and assessing their health conditions. An accurate and effective numerical model is very important for parameter identification, damage detection, and condition assessment of engineering structures. However, it is difficult to develop an accurate numerical model of a structure due to modeling errors caused by the difference between structural design and construction, the uncertainties of loads and environmental factors, and complicated boundary conditions. However, structural finite element model (FEM) updating provides an effective way to obtain a precise numerical model in each phase during the service life of a structure. Based on the field-measured data and the optimization theory, FEM updating techniques achieve a better agreement in output responses between numerical model predictions and measured results in the field. Mottershead and Friswell (1993) presented a comprehensive literature review on model updating techniques.

When using traditional model updating methods, an initial FEM of the structure is first established based on acknowledged information and then numerous iterations are performed on the entire FEM in the optimization process with a large amount of computation. The situation becomes even worse for large-scale structures with numerous degrees of freedoms. To alleviate this problem, the response surface (RS) method has been employed to generate an equivalent model to replace the FEM in model updating and damage identification process (Fang and Perera, 2009; Faravelli and Casciati, 2004; Horta, 2010). The substitution model is referred to as "meta-model" or "surrogate model" (Modak et al., 2002).

The basic idea of the RS method is to model a structure by seeking an explicit function to approximate the implicit relationship between the input parameters and output responses of the structure. The model established by the RS method is much more efficient in terms of computation amount and speed than the traditional FEM. The implementation of the RS method makes FEM updating promising in its application in the real-world structures. Structural FEM updating based on the RS method mainly contains two parts: establishing the RS models and model updating based on the constructed RS models.

Efforts have been witnessed for the RS method involved into FEM updating during the past 10 years. Marwala (2004) proposed the RS method for structural model updating by using multilayer perception to approximate the relationship between system parameters and structural responses. Fang and Perera (2011) proposed a damage identification method achieved by RS-based model updating using D-optimal designs. Deng and Cai (2010) updated a bridge model by using the genetic algorithm for optimization with the RS method for modeling the structure. The RS model was constructed by a quadratic polynomial (QP) function based on the experimental samples generated by central composite designs (CCDs). Results of numerical simulations and the application of an existing bridge showed that this method worked well and achieved reasonable physical explanations for the updated parameters. When updating a bridge FEM, Ren et al. (2010, 2011) also employed the RS method based on QP functions to model the bridge. They pointed out that it is still challenging to apply the RS method in updating the models of complex civil engineering structures where the relationship between the design parameters and the output responses is complicated and a large number of updated parameters are involved. Through a comprehensive literature review in this area, we found that almost all the reported research about the RS method for model updating is based on polynomial functions, but that based on radius basis functions (RBFs) is not much studied, which is more suitable for multivariate and complicated problems. Recently, Qin et al. (2011) updated the FEM of an airplane wing by using the RS method of a Gaussian (GA) function.

To bridge the gap in the literature, this study proposed the RS method based on RBFs for modeling large-scale structures in model updating. Herein, RBFs are used as the approximate function to model the complex and implicit relationship between design parameters and output responses. First, the RS method based on polynomial functions is briefly reviewed. Second, the RS method based on RBFs is proposed. In particular, some key issues which significantly affect the approximation accuracy of the RS method are discussed, such as the shape parameter of RBFs, selection of the input and output parameters, selection of the observed data points, and evaluation criteria. Third, the proposed method is demonstrated on a scaled cable-stayed bridge model.

2 THE RS METHOD

The RS method as a comprehensive statistical and experimental technology has been widely used to predict the relationship between the input and output of complicated systems. It can also be considered as the function fitting or interpolation of the discrete data points, which obtains the numerical model of the concerned systems based on the observed samples in the design space. One feature of this method is to express a complicated implicit function using deterministic formulas.

In this method, the approximate function, design space, and the quality of experimental samples significantly affect the modeling accuracy (Khuri and Cornell, 1987). In particular, the approximate function is arguably considered as the most important factor. The polynomial function has been mostly used as it is continuously derivable and easy for subsequent computation.

2.1 The RS method based on polynomial functions

A polynomial function with different orders can be adopted as an approximate function in the RS method. The critical step is to properly determine the order and cross-terms of the polynomial function. For most problems, the first-order and second-order polynomial functions are usually used to satisfy modeling precision and achieve a reasonable amount of calculation (Hill, 1996). The most used second-order polynomial RS model can be expressed as

$$y = \beta_0 + \sum_{i=1}^{k} \beta_i x_i + \sum_{i=1}^{k} \beta_{ii} x_i^2 + \sum_{i<j} \sum_{j} \beta_{ij} x_i x_j + \varepsilon \quad (1)$$

where β is the undetermined regression coefficient, x is the design variable, k is the number of design variables, and ε is the error term.

The number of unknown coefficients β in the second-order polynomial RS model is $(k+1)(k+2)/2$. β can be obtained by a least squares estimation. It should be noted that the number of undetermined coefficients of the polynomial RS model increase exponentially with the increase of design variables and the polynomial order, which means that more observed samples and larger calculation amount are required for the RS construction.

Theoretically, for simulation of complex problems such as a nonlinear curved surface, the RS model with higher-order polynomial functions achieves better results. However, the number of unknown regression coefficients and the amount of calculation will subsequently increase significantly, making the cost of a high-order RS model unacceptable, especially for multivariable problems.

2.2 The RS method based on RBFs

To overcome the disadvantages of the RS method based on polynomial function, the RS method based on radial basis functions (RBFs) is proposed in this section. RBFs were first proposed by Krige in 1951 in the Kriging method (Krige, 1951). They have been widely studied since the 1950s and applied in many fields, such as geodesy, geophysics, surveying and mapping, photogrammetry, remote sensing, signal processing, geography, digital terrain modeling, hydrology (Hardy, 1990), solving elliptic, parabolic, or hyperbolic partial differential equations (Fornberg and Piret, 2008), and RBF neural network (Adeli and Karim, 2000; Karim and Adeli, 2002, 2003; Ghosh et al., 2008; Savitha et al., 2009). In particular, the application of RBFs in the areas of function approximation and interpolation of scattered data has attracted considerable attention (Jackson, 1989). Compared with other approximate functions, RBFs can achieve a better performance and the advantage becomes more obvious for high-order nonlinear problems. RBFs have been validated to be the best interpolation methods compared to others by using examples of different kinds of scattered data (Frank, 1982). Powell (1991) presented a good review of the theory of RBF approximation.

Table 1
Commonly used RBFs

Name of RBF	*Expression*	*Abbreviation*
Gaussian	$\phi(r) = e^{-c \times r^2} (c > 0)$	GA
Inverse quadratic	$\phi(r) = (r^2 + c^2)^{-1}$	IQ
Multiquadratic	$\phi(r) = (r^2 + c^2)^{\frac{1}{2}}$	MQ
Inverse multiquadratic	$\phi(r) = (r^2 + c^2)^{-\frac{1}{2}}$	IMQ

2.2.1 Radial basis function. The definition of RBF proposed by Stein and Weiss (1971) is as follows: if $\|x_1\| = \|x_2\|$, the function ϕ satisfying $\phi(x_1) = \phi(x_2)$ is a RBF. It means that the RBF only depends on the function $r = \|x\|$, where $\|\cdot\|$ denotes the Euclidean norm. The most commonly used RBFs are listed in Table 1, where c is the shape parameter and $r = \|x - x_i\|$ is the Euclidean norm.

2.2.2 Modeling of RS method based on RBFs. The RS method is used to approximate a real-valued function $f(x)$ based on a finite set of values $f = \{f_1, \ldots, f_n\}$ at discrete points $X = \{\mathrm{x}_1, \ldots, x_n\} \in R^d$. Herein RBFs are chosen to construct the RS model as an approximation of the function. For positive definite RBFs such as GA, inverse quadratic (IQ), and inverse multiquadric (IMQ) functions, the RS model has the general form:

$$y = f(x) = \sum_{i=1}^{n} \lambda_i \phi(\|x - x_i\|) \, (x \in R^d, x_i \in \mathbb{X}) \quad (2)$$

where $x = \{x^1, x^2, \ldots, x^k\}$ is the vector of design variables (k is the number of updating parameters); $\mathbb{X}$ is a given set of known discrete points; $\phi(r) = \phi(\|x - x_i\|)$ is a RBF; $\|x - x_i\|$ is the Euclidean distance between an arbitrary point x and a discrete point x_i; and $\lambda = \{\lambda_1, \lambda_2, \ldots, \lambda_n\}$ is the regression coefficient vector of an RS model.

For conditional positive-definite RBFs such as multiquadric (MQ) function, some additional polynomials and constraint conditions should be adopted for the modeling of the RS model. The RS model takes the form

$$y = f(x) = \sum_{i=1}^{n} \lambda_i \phi(\|x - x_i\|) + \sum_{\alpha \le \gamma} b_\alpha x^\alpha \quad (3)$$

If $\alpha (\alpha \le \gamma)$ and $\sum_{i=1}^{n} \lambda_i x_i^\alpha = 0$, the solution to Equation (3) is unique, where γ is the order of conditional positive-definite function; α and b_α are the order and regression coefficients of the additional polynomials, respectively.

As can be seen from Equations (2) and (3), the RS model based on RBFs can be described as a weighted sum of a radially symmetric basis function based on the Euclidean distance. It should be noted that the number of regression coefficients only depends on the observed points, and almost has no relationship with the dimension of the design variable vector x. Therefore, the increase of design parameters does not require more samples. As a result, the calculation efficiency can be improved and the computational cost significantly reduced, which is very important for high dimensional and multivariate problems.

2.2.3 Selection of the shape parameter c for RBFs. As shown in Table 1, the shape parameter c is the only undetermined coefficient in a RBF, which needs to be specified by the user. It controls the "flatness" of RBFs, and is employed to adjust the curve shape of RBFs for achieving a better approximation precision.

The accuracy of approximating functions using RBFs highly depends on the selection of the shape parameter c (Frank, 1982; Carlson and Foley, 1991; Schaback, 1995). Therefore, selecting an appropriate shape parameter plays an important role when using RBFs. The value of the optimal c depends on the number and distribution of data points, the RBFs, and the precision of the computation (the condition number of the interpolation matrix) (Rippa, 1999). The shape parameter c in the RBFs application can be divided into constant c (Carlson and Foley, 1991) and variable c (Kansa and Carlson, 1992; Sarra and Sturgill, 2009). The variable c-based methods can produce more rational and accurate results. However, they are more complicated with high computational costs required. Therefore, the constant shape parameter-based methods have been widely used due to their simplicity and efficiency. In most cases, desired accuracy can be achieved with a constant shape parameter.

As a numerical illustration of the influence of the shape parameter c on function approximation, the Peaks function in MATLAB is adapted to be approximated by the RS method based on RBFs. Peaks is a bivariate function with the following form:

$$z = f(x, y) = 3(1-x)^2 e^{-x^2-(y+1)^2} \\ -10(\frac{x}{5} - x^3 - y^5)e^{-x^2-y^2} - \frac{1}{3}e^{-(x+1)^2-y^2} \quad (4)$$

It is obtained by translating and scaling Gaussian distribution with three local minimum points and three local maximum points on the concave and convex continuous surface, as shown in Figure 1a.

The RS models based on RBFs (GA and MQ) are developed for the Peaks function by using the proposed method as described in Subsection 2.2.2. Figures 1b–d display the errors distribution of the obtained RS approximation with different shaped parameters c using the same set of data points. It is clear that the magnitude and distribution of approximation errors are obviously different from each other. If a small value $c = 0.5$ is used, the major error distributes at the vicinity near the edge where the surface is supposed to be flat. Using a large value $c = 10$, the error concentrates around the maximum or minimum points of the surface. Using the value of $c = 1$, a more uniform distribution and small errors are achieved. The above discrepancy is caused by the difference in the shape of the approximation function.

To investigate the influence of different RBFs and different numbers of samples on selecting the shape parameter c, the four RBFs were used to approximate the Peaks function with various amounts of samples. From Figure 2, it can be observed that: (1) the approximation errors gradually change with the variation of the shape parameter c; (2) RBFs almost have the same minimum error, but the distribution of error is different; and (3) as the number of the observed data points increases, the approximation error is reduced dramatically and a wider range of c can be used.

It can therefore be concluded that the selection of optimal c should take account of the approximation RBFs and properties of observed data points. It is suggested that a preanalysis with different approximation functions and the shape parameter c as a continuous variable in a certain range is first conducted, and an optimal value of c can be obtained by observing the value and distribution of approximation errors.

3 SAMPLING AND EVALUATION CRITERION OF THE RS METHOD

3.1 Sample generating based on design of experiment

The selection of samples is one of the key issues for the RS approximation, significantly affecting the accuracy and the computational cost of an RS to be constructed. Based on the mathematical statistics, design of experiment (DOE) can efficiently and reasonably choose the observed samples in the global design space. With the increase of model complexity, DOE has become an essential part of the modeling process. Numerous methods of DOE were developed for different purposes. Some methods were especially proposed for the RS method, such as CCD (Montgomery, 2006), D-optimal design, and Box-Behnken design of DOE.

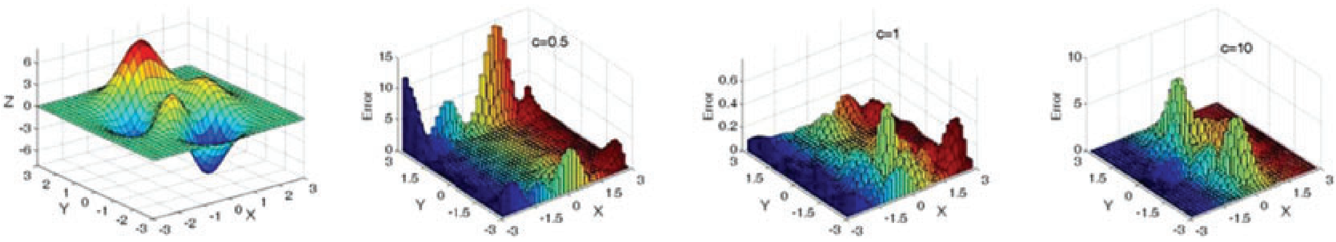

(a) The surface of Peaks (b) c=0.5 (c) c=1 (d) c=10

Fig. 1. The Peaks surface and the error distribution of the GA RS approximation. (a) Peaks function, (b) $c = 0.5$, (c) $c = 1$, and (d) $c = 10$.

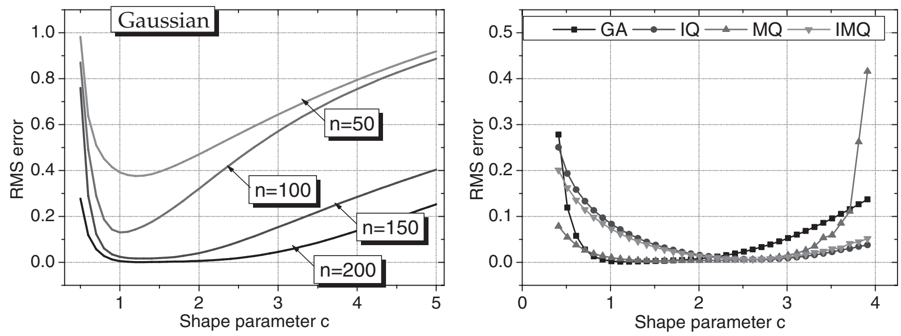

(a) GA function with various samples (b) Four RBFs with 200 samples

Fig. 2. RMS error as a function of c for the GA and MQ RS approximation defined on various amount of data points (n is the number of data points).

The CCD is adopted in this study to generate samples. The CCD samples (assume n-factor) generally consist of three components. (1) Cube points: the 2^n cube points come from a two-level full factorial design, which takes all the possible combinations of the two-level values of the parameters. (2) Axial points: the $2n$ axial points are located on a hyper-cube with the radius α. An axial point is defined by the rule that one of the parameters has the minimum or maximum value and all other parameters have their mid-levels. (3) Center point: a single point in the center is created by a nominal design. The nominal design consists of one experiment where all parameters are set to their nominal values.

It should be noted that the samples for RS modeling and accuracy evaluation are different. When selecting samples for modeling, high computation efficiency and low experiment cost are required; when selecting the samples for accuracy evaluation, a uniform and random distribution in the design space of input parameters is required. In this study, the samples for RS modeling are generated by the CCD method, and uniformly distributed pseudo-random samples are utilized for precision evaluation.

3.2 Evaluation criterion of the RS method

Many RS methods with different approximate functions and various optimization strategies are widely used in the engineering fields. Therefore, it is necessary that some evaluation criteria should be adopted to evaluate the validity and accuracy of the RS application, and the commonly used evaluation indexes are described in this section.

3.2.1 Multiple correlation coefficient R^2. The multiple correlation coefficient is used in a multiple regression analysis to assess the quality of the prediction of the dependent variable. It is an estimate of the combined influence of two or more input variables to the observed output quantity, expressed as

$$R^2 = \frac{SSR}{SSY} = \frac{\sum_{i=1}^{n} (\hat{y}_i - \bar{y})^2}{\sum_{i=1}^{n} (y_i - \bar{y})^2} \quad (5)$$

Only for a linear approximation, $SSR = SSY\text{-}SSE$, then R^2 can be further expressed as

$$R^2 = \frac{SSR}{SSY} = 1 - \frac{SSE}{SSY} = 1 - \frac{\sum_{i=1}^{n}(y_i - \hat{y}_i)^2}{\sum_{i=1}^{n}(y_i - \bar{y})^2} \quad (6)$$

where n is the number of the observed samples; y_i is the observed value; $\bar{y}$ is the average value of y_i; $\hat{y}_i$ is the predicted value by the RS model at observed points; SSR is the regression sum of squares which indicates the discreteness of y; SSY is the total sum of squares, showing the discreteness of y_i; and SSE is the error of squared sum, indicating the discreteness of y caused by random errors.

The value of R^2 closer to 1 indicates that a higher accuracy of approximation is achieved. Usually, the $0.5 \leq R^2 \leq 0.8$ defines a significant correlation between dependent and independent variables and $0.8 \leq R^2 \leq 1.0$ means a high correlation. It should be noted that only for a linear approximation, the relationship of $SSR = SSY\text{-}SSE$ can be obtained, then the R^2 in Equation (6) is constrained in the range of [0, 1]. For more general problems of nonlinearity, the R^2 of Equation (5) takes a value greater than 0.

3.2.2 Root mean squared (RMS) error. For approximation of a nonlinear function, precision can be evaluated appropriately by an RMS error, which can be written as

$$RMS = \sqrt{\frac{\sum_{i=1}^{n}(\hat{y}_i - y_i)^2}{n}} \quad (7)$$

An RMS error represents the discrepancy between measured values and predicted values of the RS model. An RS model with higher approximation accuracy achieves a smaller value of RMS error.

Obviously, the RMS error directly estimates the discrepancy between the measured value and prediction value, although the R^2 is an estimation of the correlation between dependent variables and independent variables. Compared with RMS, the R^2 has the advantage of comparing the accuracy of both diverse RS methods and different approximated problems in the range of 0∼1, but cannot exactly explain the difference between each model. For example, when R^2 is close to 1, a small change of R^2 may generate a great discrepancy of RMS error. The precisions of different models can be reflected clearly by the RMS error, but it is inconvenient to have a comparative analysis for various models. In this study, both R^2 and RMS errors are adopted to estimate the accuracy of RS approximation.

4 SIMULATION STUDY

In this study, a cable-stayed bridge model (see Figure 3) is used to illustrate the effectiveness of the RS method based on RBFs. This model was designed and manufactured according to the similarity theory based on a real-world bridge (Li et al., 2006). The scale factor is 1/40. The bridge deck and towers were made of aluminum alloy, and cables were made of steel wires with different cross-sectional areas. The bridge deck is 15.2 m long and 0.82 m wide, and the middle pylon and side pylon are 3.1 m and 1.9 m high, respectively. The total weight of aluminum alloy is about 1 ton.

4.1 Finite element model

To model the structure using the RS method, a three-dimensional FEM of this bridge model was first developed using ANSYS, as shown in Figure 4. Considering the complexity of the bridge model, ANSYS Parametric Design Language (APDL) was utilized. The bridge girders, piers, and towers were modeled by Element SOLID64, which has three translational degrees of freedom (DOFs) at each node. The bridge decks were modeled by Element SHELL63, which has both bending and membrane capabilities with six DOFs at each node (three translations and three rotations with respect to x, y, and z directions). The bridge cables were simulated by LINK10 element, which has the unique feature of a bilinear stiffness resulting in a uniaxial tension-only (or compression-only) element.

4.2 Selection of the design parameters and output characteristic parameters

There exist discrepancies between the prototype bridge and the bridge model due to the differences in materials, dimensions, boundary conditions, and connections between segments. It is worth noting that it is very complicated and difficult to exactly depict the mechanical behaviors of the connections between segments. Therefore, the adjustments of the material properties of the connection elements are considered to simulate these discrepancies. A total of 10 design parameters with potential error are selected as input parameters for the RS modeling, which are listed in Table 2. Figure 4 shows the details of connection for FEM of the bridge model.

In this methodology analysis, the first 10 natural frequencies and Modal Assurance Criteria (MACs) of mode shapes, as well as the tensions of 15 cables with different lengths and angles of inclination (see Figure 4) are selected as the output characteristic parameters. The natural frequencies and mode shapes are associated with the bridge deck modes, mid tower modes and side

Fig. 3. The 1/40 scale model of a cable-stayed bridge.

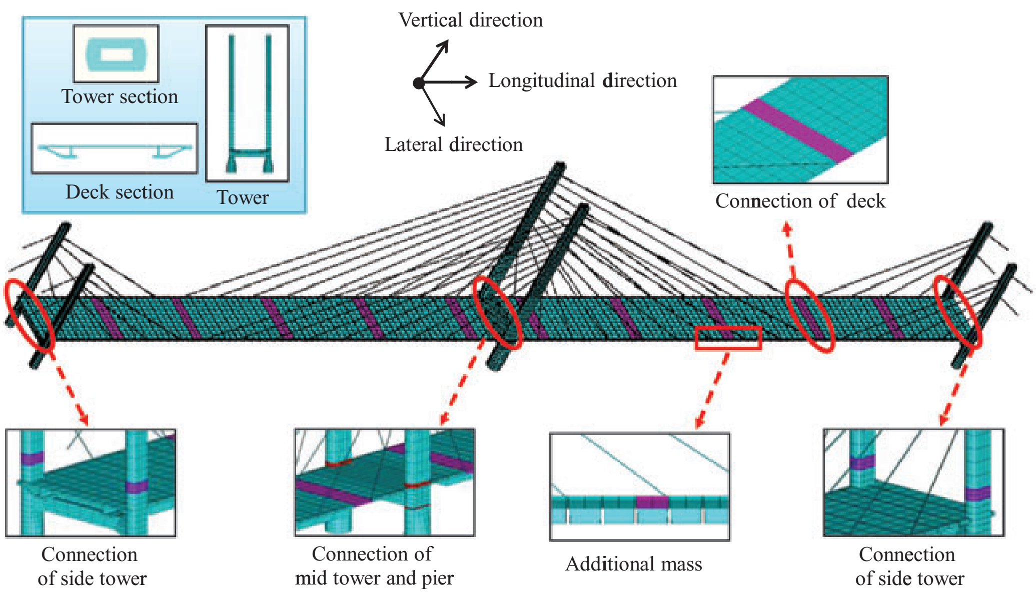

Fig. 4. The FEM of the cable-stayed bridge model.

Table 2
Selected design parameters and baseline value

Parameters	*Baseline value*	*Notation*
Young's modulus of aluminum alloy of bridge decks and pylons	52 GPa	E1
Density of aluminum alloy of bridge decks and pylons	2,700 kg/m^3	D1
Young's modulus of deck connection	52 GPa	E2
Young's modulus of pier connection	52 GPa	E3
Young's modulus of middle tower connection	52 GPa	E4
Young's modulus of side tower connection	52 GPa	E5
Mass of side tower connection	2,700 kg/m^3	D2
Young's modulus of deck cables	200 GPa	E6
Young's modulus of boundary cables	200 GPa	E7
Density of deck additional mass	7,850 kg/m^3	D3

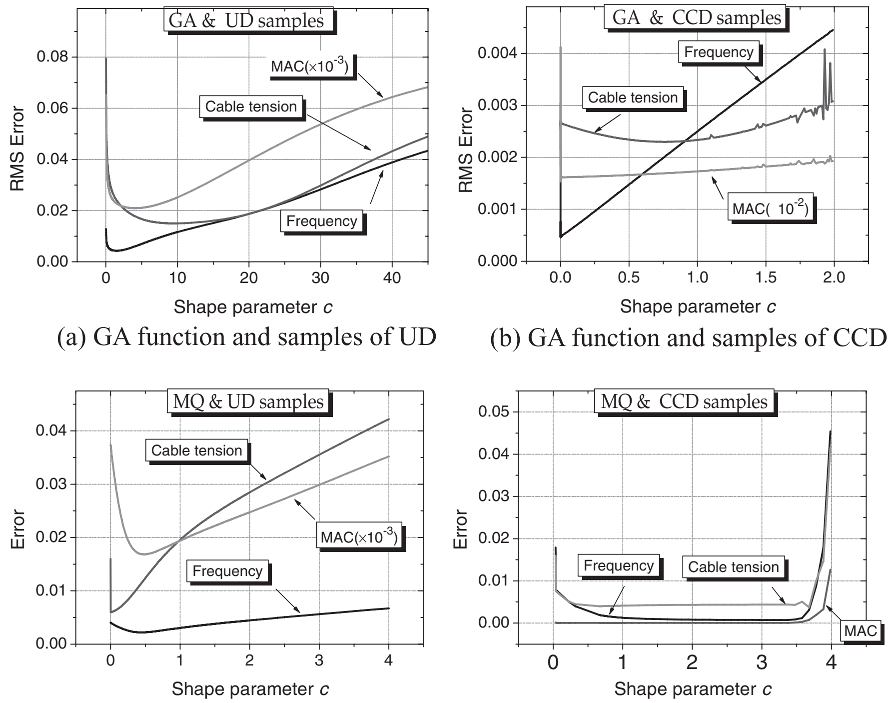

(a) GA function and samples of UD (b) GA function and samples of CCD

(c) MQ function and samples of UD (d) MQ function and samples of CCD

Fig. 5. The approximation error of RS model as a function of *c*.

tower modes. The observed cables include the bridge deck cables and boundary cables.

4.3. Selection of an optimal shape parameter *c* of RBFs for the RS method

To investigate the selection of optimal shape parameter *c* for RBF RS of approximating the implicit relationships between physical design parameters and static and dynamical output quantities of a long-span cable-stayed bridge, the same numbers of CCD and uniform distribution samples, as well as GA and MQ functions for the RS model are discussed. Figure 5 shows the approximation RMS errors in different conditions with continuous variation of *c*, and the optimal *c* is defined as the value of *c* with the minimum approximation error.

It can be seen from Figure 5 that the magnitude and distribution of approximation errors highly rely on the RBFs and observed samples. Most of the approximation errors have a continuous and smooth distribution. The error drops to a minimum and then increases with the *c* varies from zero to big value, and it is clear that an optimal *c* could be obtained when the error achieves a minimum. However, it should be noted that there are some obvious discrepancies among them. The errors of RS approximation have different trends of distribution with respect to different characteristic quantities, samples, and RBFs. Comparing Figure 5a with Figure 5b and Figure 5c with Figure 5d, shows that the error of UD samples smoothly changes and the minimum could be clearly found, but the error of CCD samples has more extreme changes when *c* takes an extremely small or relative big value. By observing the cable tension in Figure 5b, the error is dramatically disturbed when *c* takes a value near 2. One possible reason for the instability could be that the ill-conditioning occurs in calculation. By comparing Figure 5a with Figure 5c and Figure 5b with Figure 5d, it can be seen that the GA and MQ RS model are similar with respect to UD samples, but the situation is obviously different for CCD samples. The MQ RS model based on CCD samples has a long stable region for optimal *c* and stability of solution.

Based on the above discussion, it can be concluded that the optimal *c* of RBFs heavily depends on the observed samples of parameters, RBFs, and the approximated relationship. Therefore, the selection of an optimal *c* for each output characteristic quantity should be independently calculated.

4.4. Analysis of the RS method based on RBFs

In this section, the performance of the RS method based on different RBFs is evaluated for approximation. For

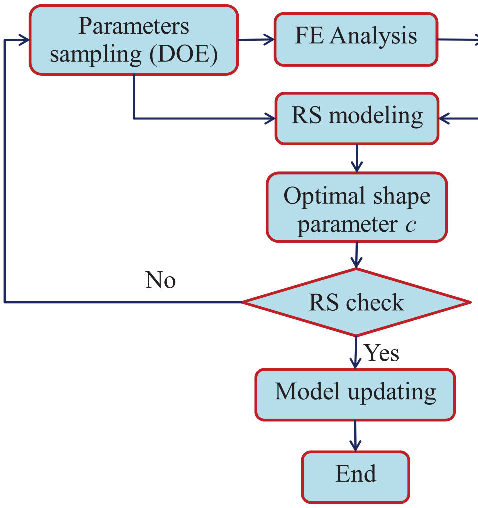

Fig. 6. The flowchart of RS modeling based on RBFs.

comparison, the RS method based on polynomial functions is also implemented. The flowchart of RS modeling and model updating based on RS methods of RBFs is shown in Figure 6.

The CCD method is adopted to generate the samples for RS modeling. Level of center points takes the baseline value, and the corner points and star points take 120% and 80% of the baseline value as the upper and lower bounds, respectively. Finite element analysis is performed and corresponding characteristic quantities can be obtained from the output responses. Then, RS models are constructed based on input samples and the output characteristic quantities. Based on uniformly distributed pseudo-random samples, accuracy of RS approximation for each output quantity is investigated with the continuous change of c from 1.0×10^{-5} to 500, and the optimal c is determined when the error reached the minimum. Meanwhile, the multiple correlation coefficient R^2 and RMS error are employed to evaluate the accuracy of RS methods. If the constructed RS models have good performance on both R^2 and RMS error, then they can be used for model updating. Otherwise, the observed samples and approximation function should be adjusted and the RS modeling procedures should be repeated.

Figure 7 presents the RS based on the GA function for the approximation of natural frequency, MAC, and cable tension with respect to the design parameters of E1 and D1. It can be seen that the relationship between design parameters and MAC is more complicated than the other two.

4.4.1 The analysis of approximating precision. Figure 8 shows the R^2 and RMS error of the first 10 natural frequencies approximation of the five discussed RS models. As can be seen from Figure 8a, R^2 of all the five RS models is nearly equal to 1, which means that all the five RS models have high approximation quality of natural frequencies. The RMS error of the 10 natural frequencies is shown in Figure 8b, which clearly displays the detail precision of each RS model. It can be observed that the error has a stable distribution, and GA model has a higher accuracy than the other four RS models. QP model also has a good precision, but IQ, MQ, and IMQ models have relatively bigger errors. Focusing on the RBFs model, GA and IMQ have better accuracies than IQ and MQ.

Figure 9 presents the R^2 and RMS error of RS models approximation for the first 10 MACs. Clearly, the approximation results are not as good as natural frequencies, and RS models of RBFs have a relatively better performance than the QP model. The R^2 and RMS error for a different MAC change dramatically. As observed in Figure 9a, the RS approximations for MACs of the 9th and 10th frequencies are almost invalid. However,

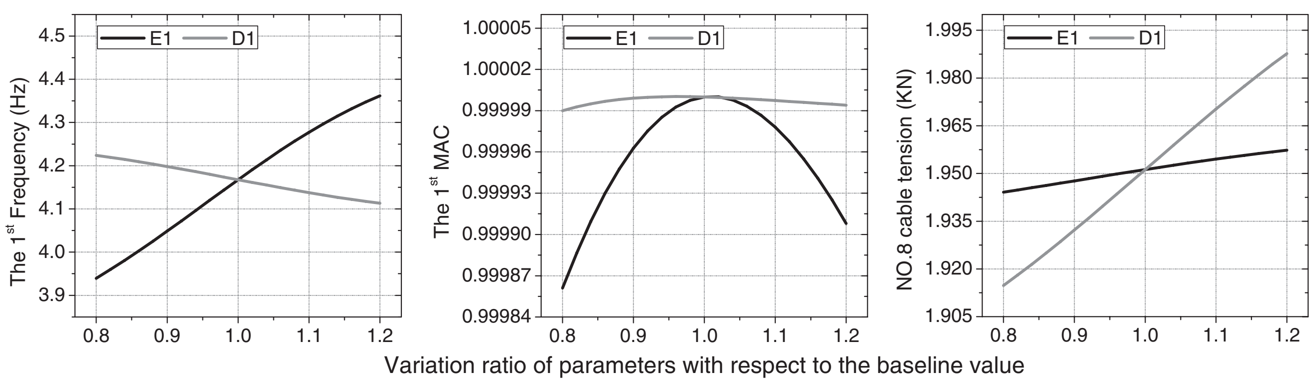

(a) The first natural frequency (b) The first MAC (c) The No. 8 cable tension

Fig. 7. The GA RS of frequency, MAC, and cable tension with respect to the design parameters of E1 and D1.

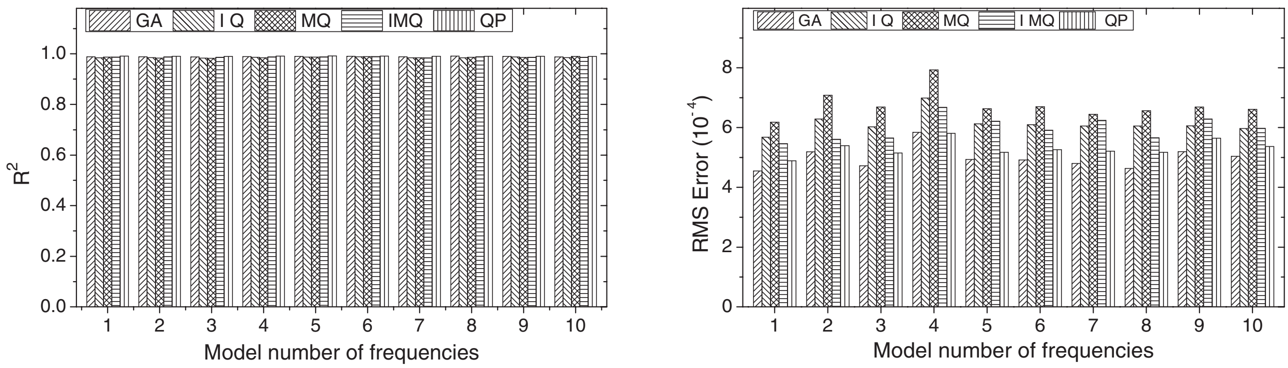

(a) The R^2 of frequencies (b) The RMS error of frequencies

Fig. 8. The RMS error and R^2 in the RS approximations of the first 10 frequencies.

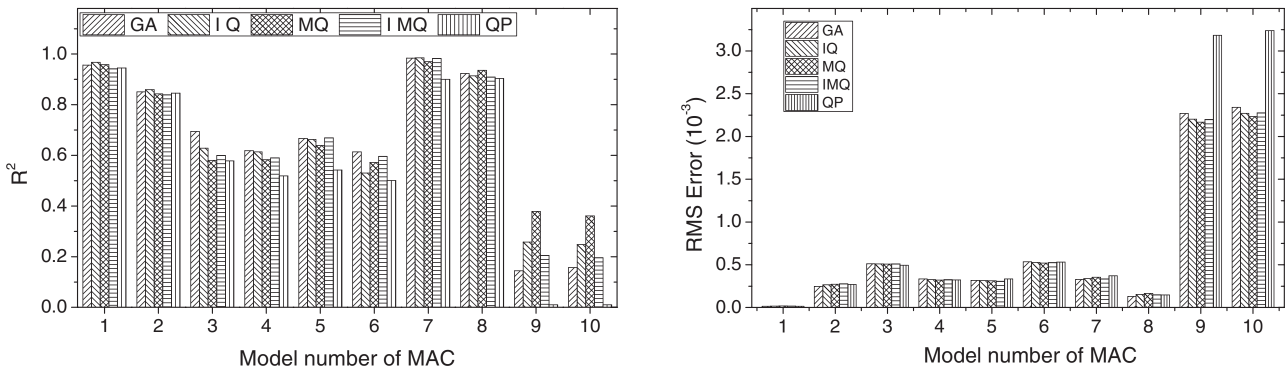

(a) The R^2 of MACs (b) The RMS error of MACs

Fig. 9. The R^2 and RMS error of the RS approximations for the first 10 MACs.

the other MACs have acceptable accuracies ($R^2 \geq 0.6$). It could be also seen in Figure 9b that the RMS errors of the 9th and 10th MAC are significantly bigger than other MACs. The 1st MAC has the lowest error with an average value of 1.6×10^{-5}, but the 10th MAC has the highest error with the mean value about 2.5.

There are two possible explanations for the high discreteness of MAC approximation. (1) MAC of mode shapes indicates the spatial vibration property of a structure, the limit of measurement points in the experimental tests makes it difficult to capture the integral characteristic of the entire structure, especially for high-order mode shapes. Usually, only the first several mode shapes can be identified with a satisfied accuracy. (2) The mode shapes of a cable-stayed bridge are more complicated due to the flexibility of this type of structure and the coupling effect between the bridge deck and the tower.

Figure 10 illustrates the R^2 and RMS error in RS approximation of 15 different cable tensions of the cable-stayed bridge. As shown in Figure 10a, all the R^2 are very close to 1, indicating that the quality of the approximations of RS methods to cable tensions is very good. The RMS errors are shown in Figure 10b, and it can be observed that the errors of the 15 cable tensions exhibit stationary distribution. Obviously, the RS method of RBFs has a better performance than the QP method; the MQ and IMQ of RBFs could obtain a higher accuracy than the GA and IQ model.

Multiple correlation coefficient R^2 is used to assess the quality of RS approximation by correlation between design parameters and response quantities. An RMS error directly estimates the gap between the observed points and the approximation value of the RS method. However, R^2 and RMS error may not reach a consistent conclusion. Because R^2 and RMS error are both very important evaluation indices for RS method approximation, it is suggested that only the RS method approximation with good performance in both R^2 and RMS error should be utilized for model updating.

4.4.2 The optimal shape parameter c. The optimal shape parameter *c* for each RS model with respect to approximated characteristic quantity is determined

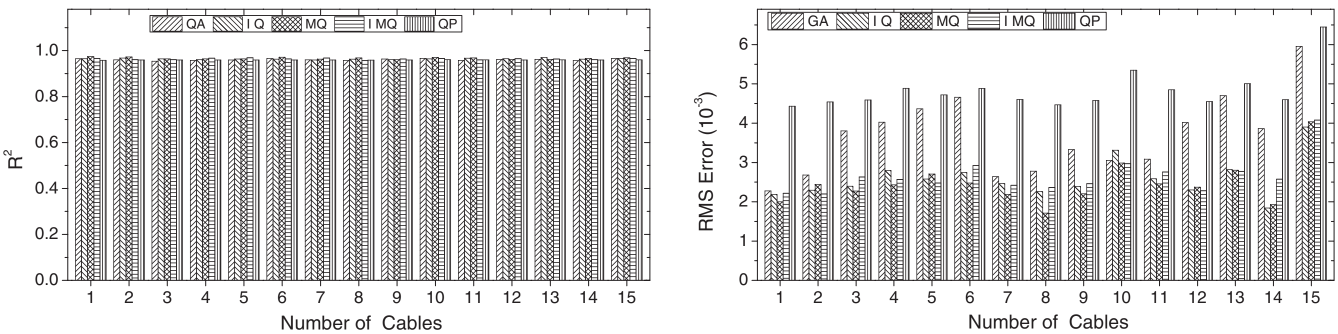

(a) The R^2 of cable tensions

(b) The RMS error of cable tensions

Fig. 10. The RMS error and R^2 in the RS approximations of 15 different cable tensions.

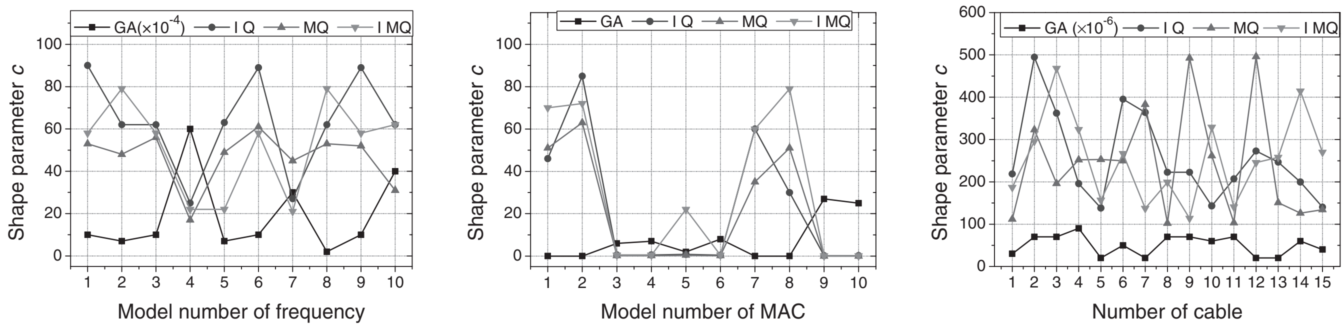

(a) Frequencies

(b) MACs

(c) Cable tensions

Fig. 11. The optimal shape parameter *c* in the RS approximations of frequencies (a), MACs (b), and cable tensions (c).

independently. Precision inspection is conducted repeatedly with the *c* monotonously and continuously changing from 0 to 500 and the optimal *c* is determined when the approximation error drops to the minimum. Figure 11 illustrates the selected optimal *c* in the RS model of RBFs approximation to natural frequencies, MACs, and cable tensions. It can be seen that the optimal *c* changes irregularly and highly depends on RBFs and approximated characteristic quantities. From Figures 11a–c, the optimal *c* of RBFs for different natural frequencies and cable tensions approximation changes stably, but MACs exhibit extreme situations where the optimal *c* takes a value that is close to 0 or a big value.

The above analysis indicates that for approximating the system of a large and complex structure by using the RS method of RBFs, the optimal *c* is highly dependent on the approximated problems and should be determined independently. The approach of precision inspection with *c* as continuously variable in a reasonable range is recommended, and then the optimal *c* can be determined as the approximation error reaches to the minimum.

4.4.3 The analysis of antinoise ability. It is well known that measurement noises on the input excitation and output response signals are unavoidable in structural experimental tests on site or in the lab, which negatively impact the experimental results. To get a better understanding of the performance of RS approximation under the situation of signals contaminated by measurement noises, GA white noise with various levels from 0% to 10% (the signal-to-noise ratio form 100 dB to 10 dB) was added to the output responses obtained from FEM analysis. Based on the noise-contaminated data, the RS models of RBFs and QP function were modeled, and precision inspection was conducted. Figure 12 shows the approximation errors for natural frequencies, MACs, and cable tensions under different levels of noises. It can be seen that noise significantly influences the approximation errors of RS methods, and the RS methods with different approximate functions are also diverse. It can be clearly seen from Figure 12 that RS method of RBFs has a better antinoise ability than RS method of QP function, and the IQ and IMQ of RBFs have a better performance than the GA and MQ function. It should be noted that the low-level noise

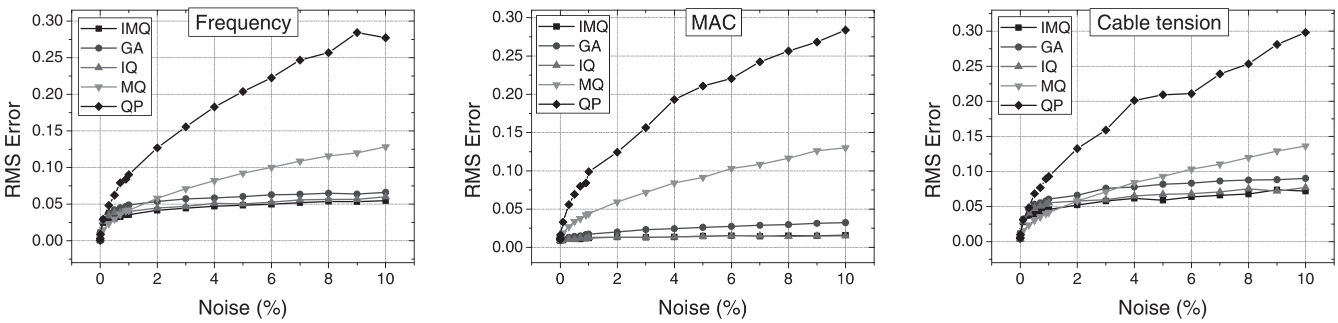

(a) Frequency (b) MAC (c) Cable tension

Fig. 12. The approximation error of RS models for frequency (a), MAC (b), and cable tension (c) under the situation of data contaminated by different degree noises.

(≤1%) significantly reduces the accuracy of approximation. However, with the increasing of noise level (≥1%), the approximation error of RBFs increases slowly although the QP still keeps a rapid growth. IQ and IMQ of RBFs have the best antinoise ability under relative high-level noise (≥1%) and QP function is the worst one.

It can be concluded that noise has considerably negative effect on the RS method for approximation of the static and dynamic properties of a long-span cable-stayed bridge. The RS based on RBFs has a better performance than the RS based on polynomial function, and the IQ and IMQ of RBFs have the best antinoise ability in the discussed five RS models.

5 MODEL UPDATING OF THE CABLE-STAYED BRIDGE MODEL

5.1 Dynamic testing of the bridge model

The dynamic testing has been conducted on the bridge model and the experimental setup is shown in Figure 13. The accelerometers are installed on both sides of the bridge deck along the longitudinal direction. There are totally 18 measurement points with symmetric distribution (14 points for vertical testing and the other 4 points for lateral testing). Two electromagnetic shakers are installed at the closure segments to excite the bridge model using white noise excitation.

Based on the dynamic testing, the first 10 natural frequencies (see Table 3) of the bridge deck are identified by eigen-system realization algorithm (ERA) combined with natural excitation technique (NExT). ERA and NExT methods for modal parameters identification have been widely used in the field testing and lab experiment of civil engineering structures.

5.2 Constructing the RS models

A cable-stayed bridge is taken as simulation study and experiment validation to demonstrate and present the procedures of the proposed RS method based on RBFs for FEM updating. According to the manufacture of the bridge physical model and limited dynamic testing data for model updating, six parameters with potential errors are selected to be updated in the model updating. They are Young's modulus of aluminum alloy (E1), density of aluminum alloy (D1), Young's modulus of deck connections (E2), the additional mass on deck (D3), Young's modulus of deck cables (E6), and Young's modulus of boundary cables (E7). Their baseline values are 52 GPa, 2,700 kg/m^3, 52 GPa, 51 kg, 200 GPa, and 200 GPa, respectively. The baseline values are usually chosen from the original construction drawings of structures. The sensitivities of the first 10 frequencies with respect to the selected six physical parameters are shown in Figure 14. It can be seen that all six parameters have considerable influence on natural frequencies, but E2 has a relatively small sensitivity compared with the other parameters.

The physical parameters are sampled by using CCD of DOE. The initial design value of each parameter is taken as the level of center points in CCD sampling, and the corner points and star points take the levels of 120% and 80% of the initial value, respectively. Then, the axial points of six-parameter CCD samples take the values of 52.43% and 147.57% of initial value. A total of 45 samples are used for RS modeling. The FEM analysis is implemented with the samples of parameters as input, and the corresponding response of natural frequencies are obtained. Then, the RS model of each natural frequency is constructed by the RS method based on GA function. GA RBF is used for the RS modeling because it has a good performance on approximating the relationships between natural frequencies and physical parameters as discussed in Section 4.4.

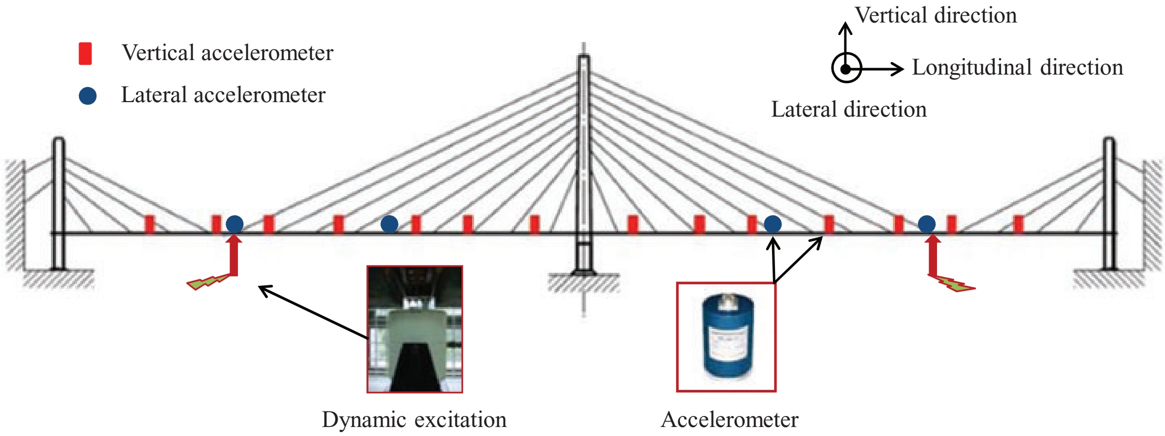

Fig. 13. Dynamic testing of the bridge physical model.

Table 3
The identified natural frequencies (Hz)

Order	*Description*	*Value*
1	The first order of vertical mode	4.014
2	The second order of vertical mode	8.839
3	The third order of vertical mode	10.822
4	The first order of lateral mode	10.963
5	The fourth order of vertical mode	11.857
6	The fifth order of vertical mode	14.312
7	The second order of lateral mode	15.075
8	The sixth order of vertical mode	16.344
9	The seventh order of vertical mode	21.926
10	The eighth order of vertical mode	22.962

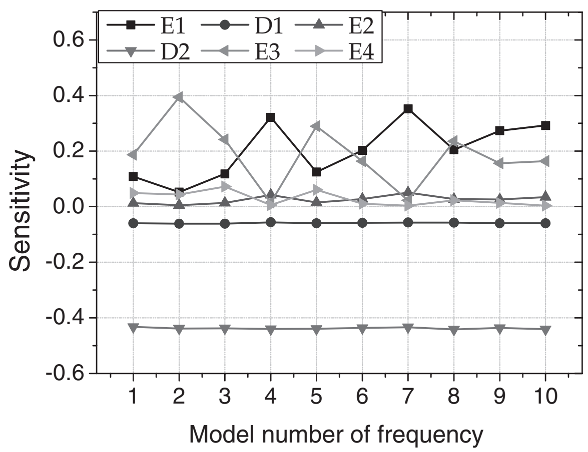

Fig. 14. Sensitivity of frequencies to physical parameters.

Accuracies of RS approximation of the 10 natural frequencies are investigated with the continuous change of shape parameter c from 1.0×10^{-5} to 10, and the optimal c is determined when the error reaches to the minimum.

Table 4
Optimal c of RBF RS models of frequencies

Frequency no.	1	2	3	4	5	6	7	8	9	10
Optimal c (10^{-4})	8.3	7.5	8.6	8.9	6.5	8.3	5.7	6.9	8.7	6.9

The optimal c for the RS models of frequencies is listed in Table 4. The multiple correlation coefficient R^2 and RMS error are employed to evaluate the constructed RS models as shown in Figure 15. It can be seen that all the R^2 are very close to 1 and the RMS errors are very small (10^{-5}), then it can be concluded that the RS models have good quality and accuracy of approximation, and can be used for the following model updating.

5.3 Model updating based on numerical simulation

Numerical simulation of model updating on the bridge model is carried out to test the validity of the proposed approach. A random change is taken to the physical parameters based on the initial design values in design space and corresponding natural frequencies are obtained from the FEM analysis as target (measured) characteristic information for model updating. An objective function is built up using the residuals between the measured and the RS predicted natural frequencies

$$Obj(X) = \sum_{i=1}^{N} w_i \left(\frac{f_{ai} - f_{ei}}{f_{ei}} \right)^2 \tag{8}$$

where f_{ei} and f_{ai} are the ith measured and RS predicted natural frequencies respectively; w_i is the weight coefficient of ith natural frequency; N is the number of modes involved; and X is the vector of design parameters.

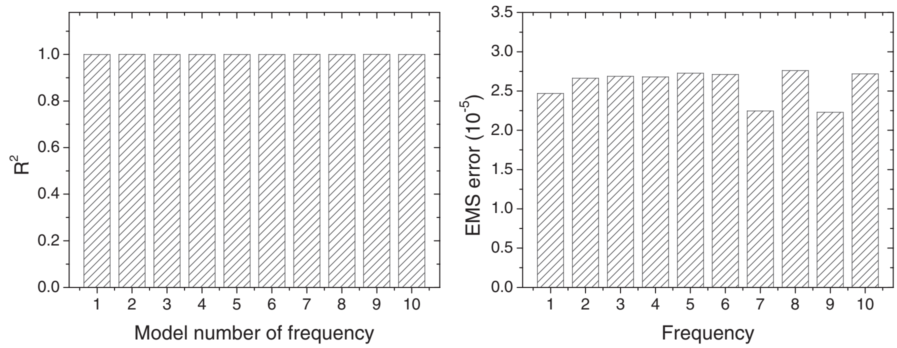

(a) The multiple correlation coefficient R^2 (b) Root mean squared (RMS) error

Fig. 15. The R^2 and RMS error of the GA RS models of the natural frequencies.

Table 5
The model updating results of cable-stayed bridge in numerical simulation

Parameter	*Notation*	*Initial value*	*Target value*	*Updated value*	*Error (%)*
Young's modulus of aluminum alloy (GPa)	E1	52	49.92	49.95	0.06
Density of aluminum alloy (kg/m^3)	D1	2,700	2,835.00	2,832.84	−0.08
Young's modulus of deck connection (GPa)	E2	52	44.20	44.61	0.91
The additional mass on deck (kg/m^3)	D3	7,850	8,007.00	7,991.61	−0.19
Young's modulus of deck cables (GPa)	E6	200	190.00	190.22	0.12
Young's modulus of boundary cables (GPa)	E7	200	180.00	180.70	0.39

Then, FEM updating is implemented based on the constructed RS models and objective function (values of all the weight coefficients are taken as 1) by using a genetic algorithm (Sgambi et al., 2012; Putha et al., 2012). The updated results of numerical simulation are summarized in Table 5. The updated values of the parameters are very close to the true values with a maximum error of only 0.91%. The comparison of the 10 natural frequencies which are employed for model updating can be found in Table 6. The updated values and true values of natural frequencies are almost the same. Therefore, the numerical simulation indicates that the performance of the RS method of RBFs for model updating of a cable-stayed bridge is very encouraging.

Table 6
Comparison of natural frequencies after model updating in numerical simulation

Order	*Target value (Hz)*	*Updated value (Hz)*	*Error (%)*
1	4.0349	4.0350	0.0015
2	8.9033	8.9038	0.0051
3	10.8117	10.8121	0.0038
4	11.6142	11.6129	−0.0114
5	11.6060	11.6045	−0.0134
6	14.0175	14.0174	−0.0006
7	14.8664	14.8684	0.0137
8	15.5512	15.5523	0.0071
9	21.0115	21.0133	0.0087
10	21.5404	21.5368	−0.0167

5.4 Model updating based on experimental data

Model updating is also carried out on the bridge model based on experimental data. The objective function is built up using Equation (8). The weight coefficients of the objective function are taken as [3 3 3 1 2 2 2 1 1 1] for the first 10 natural frequencies. The lower order natural frequencies take relatively larger weight coefficients than higher natural frequencies because the lower natural frequencies of structures can be identified with high accuracy, and lateral model (4th mode) of bridge deck takes a small weight coefficient because the testing and identification are not very reliable due to the fact that few sensors are used. Model updating is optimized by using a genetic algorithm. The lower and upper bounds for the six parameters are set to be [90%; 90%; 60%; 90%; 90%; 60%] and [105%; 105%; 100%; 105%; 105%; 110%] of initial design values.

Table 7
Results of model updating based on tested data

Parameter	*Initial value*	*Updated value*	*Difference (%)*
E1 (GPa)	52	50.76	−2.39
D1 (kg/m^3)	2,700	2,772.90	2.70
E2 (GPa)	52	45.77	−11.99
D3 (kg/m^3)	7,850	7,930.07	1.02
E6 (GPa)	200	194.58	−2.71
E7 (GPa)	200	157.00	−21.50

Table 8
Error of natural frequencies after model updating based on tested data

Order	*Measured value (Hz)*	*Updated value (Hz)*	*Error (%)*
1	4.014	4.045	0.760
2	8.839	8.971	1.493
3	10.822	10.824	0.022
4	10.963	11.722	6.922
5	11.857	11.662	−1.648
6	14.312	14.167	−1.012
7	15.075	15.033	−0.280
8	16.344	15.722	−3.806
9	21.926	21.247	−3.096
10	22.962	21.830	−4.932

The results of model updating are listed in Table 7. As can be seen from the table, the Young's modulus of aluminum alloy (E1) and the additional mass on deck (D3) have been decreased because the material and dimension are slightly smaller than real values. The increase of the density of aluminum alloy (D1) is reasonable because the connections of deck and cables increase the mass on the deck. The large decrease of Young's modulus of deck connection (E2) can be predictable because the stiffness of the connection of deck is weaker than the intact deck. The decrease in Young's modulus of deck cables (E6) and boundary cables (E7) could be attributed to the weakness of the connection and boundary condition at the ends of cables.

The comparison of the natural frequencies between measured values and updated values after model updating can be seen from Table 8. The results are acceptable with almost all errors below 5% except the first-order lateral mode with the largest error 6.92%. However, it is obvious that the results are not so good as numerical simulation. The gap between tested values and updated values cannot be closed because of the existing error in testing and identifying of the physical model experiments. The relatively big errors in lateral modes and higher order modes are consistent with the practical cases in field testing.

6 CONCLUSIONS

The article proposed the RS method based on RBFs to model large-scale structures for model updating. The complicated and implicit relationships between design parameters and output characteristic parameters of cable-stayed bridges are employed to investigate the performance of the RS method based on RBFs. A three-dimensional FEM of a scaled cable-stayed bridge model is established for numerical simulation. The design parameters of interest include global and local physical parameters, and the output response quantities consist of static properties and dynamic features of cable-stayed bridges. To successfully apply the RS method of RBFs for model updating of cable-stayed bridges, appropriate RBF for different approximated relationship should be first determined. Meanwhile, the selection of an optimal c of RBFs is very important, which heavily depends on the modeling samples, RBFs, and the approximated relationship.

The simulation study of a cable-stayed bridge shows that all of the RS models have high accuracy for approximation of frequencies, MACs and cable tensions. RS model of RBFs exhibits a better performance than polynomial RS model. It can also be found that different RS models have different performance for various approximated problems. GA RBF has the highest precision for frequencies approximation, but MQ and IMQ of RBFs have a better accuracy for cable tension approximation. For MAC, RBFs are almost the same but slightly better than a polynomial function. Concerning the antinoise ability, the RS method based on RBFs has remarkable advantages over the QP model.

It is demonstrated that the increase of design space dimensions (model variables) does not require adding more samples for RBF RS construction. Therefore, the RS method based on RBFs has the potential to apply in more complicated, high dimensional and multivariate problems. The approach and strategies proposed in this article have been applied to the model updating of a cable-stayed bridge model. Simulation study and experimental verification indicate that this method works well and can be easily implemented in practice for model updating of complicated bridges such as long-span cable-stayed bridges.

ACKNOWLEDGMENTS

This research is supported by the Project of National Key Technology R & D Program (China) 2011BAK02B01 and the National Basic Research Program of China (973 Program) 2013CB036305. The authors would like to thank the Editor and the anonymous reviewers for their constructive comments and valuable suggestions to improve the quality of the article.

REFERENCES

Adeli, H. & Jiang, X. (2006), Dynamic fuzzy wavelet neural network model for structural system identification, *Journal of Structural Engineering*, **132**(1), 102–11.

Adeli, H. & Jiang, X. (2009), *Intelligent Infrastructure – Neural Networks, Wavelets, and Chaos Theory for Intelligent Transportation Systems and Smart Structures*, CRC Press, Taylor & Francis, Boca Raton, FL.

Adeli, H. & Karim, A. (2000), Fuzzy-wavelet RBFNN model for freeway incident detection, *Journal of Transportation Engineering*, **126**(6), 464–71.

Adeli, H. & Kim, H. (2009), *Wavelet-Based Vibration Control of Smart Buildings and Bridges*, CRC Press, Taylor & Francis, Boca Raton, FL.

Carlson, R. E. & Foley, T. A. (1991), The parameter R^2 in multiquadric interpolation, *Computers & Mathematics with Applications*, **21**(9), 29–42.

Deng, L. & Cai, C. S. (2010), Bridge model updating using response surface method and genetic algorithm, *Journal of Bridge Engineering*, **15**(5), 553–64.

Fang, S. E. & Perera, R. (2009), A response surface methodology based damage identification technique, *Smart Materials and Structures*, **18**(6), 1–14.

Fang, S. E. & Perera, R. (2011), Damage identification by response surface based model updating using D-optimal design, *Mechanical Systems and Signal Processing*, **25**(2), 717–33.

Faravelli, L. & Casciati, S. (2004), Structural damage detection and localization by response change diagnosis, *Structural Safety and Reliability*, **6**(2), 104–115.

Fornberg, B. & Piret, C. (2008), On choosing a radial basis function and a shape parameter when solving a convective PDE on a sphere, *Journal of Computational Physics*, **227**, 2758–80.

Franke, R. (1982), Scattered data interpolation: test of some methods, *Mathematics of Computation*, **38**(157), 181–200.

Gangone, M. V., Whelan, M. J. & Janoyan, K. D. (2011), Wireless monitoring of a multi-span bridge superstructure for diagnostic load testing and system identification, *Computer-Aided Civil and Infrastructure Engineering*, **26**(7), 569–79.

Ghosh-Dastidar, S., Adeli, H. & Dadmehr, N. (2008), Principal component analysis-enhanced cosine radial basis function neural network for robust epilepsy and seizure detection, *IEEE Transactions on Biomedical Engineering*, **55**(2), 512–18.

Hampshire, T. A. & Adeli, H. (2000), Monitoring the behavior of steel structures using distributed optical fiber sensors, *Journal of Constructional Steel Research*, **53**(5), 267–81.

Hardy, R. L. (1990), Theory and applications of the multiquadric-biharmonic method, *Computers & Mathematics with Applications*, **19**, 163–208.

Hill, W. J. & Hunter, W. G. (1966), A review of response surface methodology: a literature survey, *Technometrics*, **8**(4), 571–90.

Horta, L. H., Reaves, M. C., Buehrle, R. D., Templeton, J. D., Lazor, D. R., Gaspar, J. L., Parks, R. A. & Bartolotta, P. A. (2010), Finite element model calibration approach for Ares I-X, in *Proceedings of IMAC XXVIII*, Jacksonville, FL, 1037–54.

Jackson, I. R. H. (1989), *Radial Basis Functions: A Survey and New Results*, *The Mathematics of Surfaces, III*, Oxford University Press, Oxford, UK.

Jafarkhani, R. & Masri, S. F. (2011), Finite element model updating using evolutionary strategy for damage detection, *Computer-Aided Civil and Infrastructure Engineering*, **26**(3), 207–24.

Jiang, X. & Adeli, H. (2005), Dynamic wavelet neural network for nonlinear identification of highrise buildings, *Computer-Aided Civil and Infrastructure Engineering*, **20**(5), 316–30.

Jiang, X. & Adeli, H. (2007), Pseudospectra, MUSIC, and dynamic wavelet neural network for damage detection of highrise buildings, *International Journal for Numerical Methods in Engineering*, **71**(5), 606–29.

Jiang, X. & Adeli, H. (2008a), Dynamic fuzzy wavelet neuroemulator for nonlinear control of irregular highrise building structures, *International Journal for Numerical Methods in Engineering*, **74**(7), 1045–66.

Jiang, X. & Adeli, H. (2008b), Neuro-genetic algorithm for nonlinear active control of highrise buildings, *International Journal for Numerical Methods in Engineering*, **75**(7), 770–86.

Jiang, X., Mahadevan, S. & Adeli, H. (2007), Bayesian wavelet packet denoising for structural system identification, *Structural Control and Health Monitoring*, **14**(2), 333–56.

Kansa, E. J. & Carlson, R. E. (1992), Improved accuracy of multiquadric interpolation using variable shape parameters, *Computers & Mathematics with Applications*, **24**(12), 99–120.

Karim, A. & Adeli, H. (2002), Comparison of fuzzy-wavelet radial basis function neural network freeway incident detection model with California algorithm, *Journal of Transportation Engineering*, **28**(1), 21–30.

Karim, A. & Adeli, H. (2003), Radial basis function neural network for work zone capacity and queue estimation, *Journal of Transportation Engineering*, **129**(5), 494–503.

Khuri, A. I. & Cornell, J. A. (1987), *Response Surface Designs and Analysis*, Marcel Dekker, Inc., New York.

Krige, D. G. (1951), A statistical approach to some basic mine valuation problems on the Witwatersrand, *Journal of the Chemical, Metallurgical and Mining Society of South Africa*, **52**(6), 119–39.

Li, H., Huang, Y., Chen, W. L., Ma, M. L., Tao, D. W. & Ou, J. P. (2011a), Estimation and warning of fatigue damage of FRP stay cables based on acoustic emission technique and fractal theory, *Computer-Aided Civil and Infrastructure Engineering*, **26**(7), 500–12.

Li, H., Huang, Y., Ou, J. & Bao, Y. (2011b), Fractal dimension-based damage detection method for beams with a uniform cross-section, *Computer-Aided Civil and Infrastructure Engineering*, **26**(3), 190–206.

Li, H., Ou, J. & Zhao, X. (2006), Structural health monitoring system for the Shandong Binzhou Yellow River Highway Bridge, *Computer-Aided Civil and Infrastructure Engineering*, **21**(4), 306–17.

Marwala, T. (2004), Finite element model updating using response surface method. Collection of Technical Papers – *AIAA/ASME/ASCE/AHS/ASC Structures, Structural Dynamics and Materials Conference*, Vol. 7, pp. 5165–73.

Modak, S. V., Kundra, T. K. & Nakra, B. C. (2002), Comparative study of model updating methods using simulated experimental data, *Computers & Structures*, **80**(5–6), 437–47.

Montgomery, D. C. (2006), *Design and Analysis of Experiments*, John Wiley & Sons, Inc., New York.
Mottershead, J. E. & Friswell, M. I. (1993), Model updating in structural dynamics: a survey, *Journal of Sound and Vibration*, **167**(2), 347–75.
Ou, J. P. (2004), Advances on vibration control and health monitoring of civil infrastructures in mainland China, in *International Symposium on Network and Center-Based Research for Smart Structures Technologies and Earthquake Engineering*, Tokyo, Japan, 6–10.
Ou, J. P. & Li, H. (2010), Structural health monitoring in mainland China-review and future trends, *Structural Health Monitoring*, **9**(3), 219–31.
Park, H. S., Lee, H. M. & Adeli, H. (2007), A new approach for health monitoring of structures: terrestrial laser scanning, *Computer-Aided Civil and Infrastructure Engineering*, **22**(1), 19–30.
Powell, M. J. D. (1991), *The Theory of Radial Basis Function Approximation in 1990*, Oxford University Press, Oxford, UK.
Putha, R., Quadrifoglio, L. & Zechman, E. (2012), Comparing ant colony optimization and genetic algorithm approaches for solving traffic signal coordination under oversaturation conditions, *Computer-Aided Civil and Infrastructure Engineering*, **27**(1), 14–28.
Qiao, L., Esmaeily, A. & Melhem, H. G. (2012), Signal pattern-recognition for damage diagnosis in structures, *Computer-Aided Civil and Infrastructure Engineering*, **27**(9), 699–710.
Qin, Y., Kong, X. & Luo, W. (2011), Finite element model updating of airplane wing based on Gaussian radial basis function response surface, *Journal of Beijing University of Aeronautics and Astronautics*, **37**(11), 1465–70.
Ren, W. X. & Chen, H. B. (2010), Finite element model updating in structural dynamics by using the response surface method, *Engineering Structures*, **32**(8), 2455–65.
Ren, W. X., Fang, S. E. & Deng, M. Y. (2011), Response surface based finite element model updating using structural static responses, *Journal of Engineering Mathematics*, **137**(4), 248–57.
Rippa, S. (1999), An algorithm for selecting a good value for the parameter e in radial basis function interpolation, *Advances in Computational Mathematics*, **11**(2), 193–210.
Sarra, S. A. & Sturgill, D. (2009), A random variable shape parameter strategy for radial basis function approximation methods, *Engineering Analysis with Boundary Elements*, **33**(11), 1239–45.
Savitha, R., Suresh, S. & Sundararajan, N. (2009), A fully complex-valued radial basis function network and its learning algorithm, *International Journal of Neural Systems*, **19**(4), 253–67.
Schaback, R. (1995), Error estimates and condition numbers for radial basis function interpolation, *Advances in Computational Mathematics*, **3**, 251–64.
Sgambi, L., Gkoumas, K. & Bontempi, F. (2012), Genetic algorithms for the dependability assurance in the design of a long span suspension bridge, *Computer-Aided Civil and Infrastructure Engineering*, **27**(9), 655–75.
Stein, E. M. & Weiss, G. (1971), *Introduction to Fourier Analysis on Euclidean Space*, Princeton University Press, Princeton, NJ.
Talebinejad, I., Fischer, C. & Ansari, F. (2011), Numerical evaluation of vibration based methods for damage assessment of cable stayed bridges, *Computer-Aided Civil and Infrastructure Engineering*, **26**(3), 239–51.
Xia, Y., Ni, Y. Q., Zhang, P., Liao, W. Y. & Ko, J. M. (2011), Stress development of a super-tall structure during construction: numerical analysis and field monitoring verification, *Computer-Aided Civil and Infrastructure Engineering*, **26**(7), 542–59.
Xiang, J. & Liang, M. (2012), Wavelet-based detection of beam cracks using modal shape and frequency measurements, *Computer-Aided Civil and Infrastructure Engineering*, **27**(6), 439–54.